





Article

Solution-Processed OLED Based on a Mixed-Ligand Europium Complex

Makarii I. Kozlov ^{1,2}, Kirill M. Kuznetsov ², Alexander S. Goloveshkin ³, Andrei Burlakin ⁴, Maria Sandzhieva ⁴, Sergey V. Makarov ^{4,5}, Elena Ilina ⁶ and Valentina V. Utochnikova ^{1,2,*}

¹ Department of Chemistry, M.V. Lomonosov Moscow State University, 1/3 Leninskie Gory, 119991 Moscow, Russia

² Department of Material Sciences, M.V. Lomonosov Moscow State University, 1/3 Leninskie Gory, 119991 Moscow, Russia

³ A. N. Nesmeyanov Institute of Organoelement Compounds, Vavilova St. 28, 119334 Moscow, Russia

⁴ School of Physics and Engineering, ITMO University, Lomonosova 9, 197101 St. Petersburg, Russia

⁵ Qingdao Innovation and Development Center, Harbin Engineering University, Qingdao 266000, China

⁶ Institute of Chemistry and Chemical-Pharmaceutical Technologies, Altai State University, Prospekt Lenina 61, 656049 Barnaul, Russia

* Correspondence: valentina.utochnikova@gmail.com

Abstract: An approach to increase the efficiency of europium-based OLEDs was proposed through the formation of a mixed-ligand complex. The design of a series of europium complexes, together with an optimization of the solution deposition, including the host selection, as well as the variation of the solvent and deposition parameters, resulted in a noticeable increase in OLED luminance. As a result, the maximum luminance of the Eu-based OLED reached up to 700 cd/m², which is one of the highest values for an Eu-based solution-processed OLED. Finally, its stability was investigated.

Keywords: OLED; electroluminescence; europium; mixed-ligand complex; lifetime



Citation: Kozlov, M.I.; Kuznetsov, K.M.; Goloveshkin, A.S.; Burlakin, A.; Sandzhieva, M.; Makarov, S.V.; Ilina, E.; Utochnikova, V.V. Solution-Processed OLED Based on a Mixed-Ligand Europium Complex. *Materials* **2023**, *16*, 959. <https://doi.org/10.3390/ma16030959>

Academic Editor: Jianwu Shi

Received: 4 December 2022

Revised: 10 January 2023

Accepted: 12 January 2023

Published: 19 January 2023



Copyright: © 2023 by the authors. Licensee MDPI, Basel, Switzerland. This article is an open access article distributed under the terms and conditions of the Creative Commons Attribution (CC BY) license (<https://creativecommons.org/licenses/by/4.0/>).

1. Introduction

Despite the rapid development of organic light-emitting diode (OLED) technology, several important issues remain to be solved. Among them, narrowing the luminescence bands of the OLEDs is particularly important [1] due to the swift acceleration of wearable electronics development [2,3], including in tissue oximetry [4], where narrow-band luminescence simplifies the detection and fits into the transparency window of biological tissues [5]. The ultimate solution to this problem is the use of lanthanide coordination compounds (Ln CCs) with extremely narrow luminescence bands (<10 nm) [6]. In particular, europium complexes with their high quantum yields (PLQYs) and red emission (~615 nm) are of interest. However, the peculiarities of Ln-based OLEDs [7], particularly their long exciton lifetime (τ) [8], still result in low luminance and efficiencies of OLEDs based on Eu CCs [9]. This makes it an urgent task to search for new materials, as well as to optimize the OLED deposition parameters, to which Eu CCs with their long lifetimes are particularly sensitive.

Most commercially available OLEDs are produced using vacuum thermal evaporation (VTE) due to the higher luminance and efficiency of OLEDs produced this way, resulting from the higher purity of the deposited films [10]. At the same time, VTE has some disadvantages, including the impossibility of using non-volatile compounds, high complexity, cost of the technological process, and the complexity of optimization of the material co-evaporation [11]. Thus, the development of solution-processed methods is itself an important task.

However, solution deposition is always associated with fast degradation [10,12,13], which is particularly harmful to Ln-based OLEDs, whose long excited-state lifetimes already facilitate degradation. As a result, the highest luminance obtained for solution-processed lanthanide-based OLEDs is very low, while their degradation has not been studied at all.

At the same time, for some materials, it has already been possible to obtain spin-coated (SC) OLEDs, which are only slightly inferior to similar VTE devices [13], due to the SC film deposition process, i.e., the optimal solvent, rotation rate, and annealing conditions. Mao et al. reported similar OLED performance for VTE-deposited and SC films [14], while Feng et al. reported that SC films of TPD (tri-methylphenyl diamine) were superior to the VTE-deposited ones, being much smoother and denser [15]. For Ln-based OLEDs, this was rarely studied, but we have recently demonstrated [16] that solution-deposited films of Eu CCs are denser than VTE-deposited films, which resulted in a decrease in the turn-on voltage.

In this paper, SC deposition of the emission layers based on europium mixed-ligand complexes was studied and optimized. Their photophysical properties, depending on the host material and deposition conditions, were studied, aiming at obtaining the highest PLQY/ τ ratio, and the optimized films were tested in OLEDs. As the object of study, mixed-ligand europium complexes Eu(dik)₃DPPZ with dipyrrodo [3,2-a:2'-c,3'-c]phenazine (DPPZ) β -diketones (dik = tta (thenoyltrifluoroacetone), dbm (dibenzoylmethane), and btfa (benzoyltrifluoroacetone)) were used, since DPPZ-containing β -diketonates demonstrated the record luminance of electroluminescence (EL) [17].

2. Materials and Methods

All solvents and chemicals were purchased from commercial sources.

Powder X-ray diffraction data (PXRD) were collected using Bruker D8 Advance (Karlsruhe, Germany) [λ (Cu-K α) = 1.5418 Å; Ni filter] with a step size of 0.020°.

A suitable single crystal of [Eu(btfa)₃DPPZ] (C₄₈H₂₈EuF₉N₄O₆) was selected and mounted on a Bruker Quest diffractometer. The crystal was kept at 100 K during data collection. Using Olex2 [18], the structure was solved with the XS [19] structure solution program using Direct Methods and refined with the XL [19] refinement package using Least Squares minimization.

Crystal Data for [Eu(btfa)₃DPPZ] (C₄₈H₂₈EuF₉N₄O₆, M = 1079.70 g/mol): tetragonal, space group *P4/n* (no. 85), a = 27.5502(3) Å, c = 11.6190(3) Å, V = 8819.0(3) Å³, Z = 8, T = 100 K, μ (MoK α) = 1.515 mm⁻¹, D_{calc} = 1.626 g/cm³, 52,490 reflections measured (3.804° ≤ 2 θ ≤ 56.584°), 10,940 unique (R_{int} = 0.0624, R_{sigma} = 0.0531), which were used in all calculations. The final R1 was 0.0563 (I > 2 σ (I)) and wR2 was 0.1235 (all data).

CCDC 2223863 contains the supplementary crystallographic data for this paper. These data can be obtained free of charge from The Cambridge Crystallographic Data Centre via <http://www.ccdc.cam.ac.uk> (deposition date 2 December 2022).

Thermal analysis was carried out on an STA 409PC Luxx thermoanalyzer (NETZSCH, Selb, Germany) in the temperature range of 20–1000 °C in air, at a heating rate of 10 (°)/min. The evolved gases were simultaneously monitored during the TA experiment using a coupled QMS 403C Aeolos quadrupole mass spectrometer (NETZSCH, Selb, Germany). The mass spectra were registered for the species with the following *m/z* values: 18 (corresponding to H₂O), 44 (corresponding to CO₂), 46 (corresponding to C₂H₅OH), and 127 (corresponding to I).

The IR spectra were recorded on a Nicolet iS50 FTIR Spectrometer as a powder at ATR (Thermo Scientific, Waltham, MA, USA).

Photoluminescence spectra were recorded using a Fluoromax Plus (HORIBA, Piscataway, NJ, USA) spectrometer at room temperature; excitation was performed through a ligand, and the absolute method in the integration sphere was used.

2.1. OLED Manufacture

Prepatterned indium tin oxide coating with 15 Ohm/sq on the glass substrates (Kaivo LTD) were used as anodes. The substrates were cleaned by three-step ultrasonication in deionized water, acetone, and isopropanol for 15 min each followed by drying with airflow. Then a 20 min UV treatment was performed to remove residual organic impurities.

Hole injection layer PEDOT-PSS (poly(3,4-ethylenedioxythiophene):poly(styrenesulfonate) (Ossila Al-4083) was spin-coated on cleaned ITO glass substrates at 3000 rpm for 1 min with the following annealing process at 140 °C for 10 min in the air. Then a 20 nm thick hole-transporting poly-TPD (Ossila) solution was spin-coated from 5 mg/mL solution in chlorobenzene at 1500 rpm for 1 min and dried at 120 °C for 10 min in the nitrogen-filled glovebox. Afterward, a 30 nm thick emission layer was spin-coated from THF (Eu(dik)₃DPPZ:CBP 1:3, total c = 5 g·L⁻¹) at 1500 rpm for 1 min with further annealing at 80 °C for 10 min.

Finally, the substrates were transferred into a MB-ProVap 5G vacuum deposition system. The ~20 nm thick electron-transporting/hole-blocking layer TPBi (Lumtec) was thermally evaporated followed by a ~1 nm thick LiF layer and 100 nm thick aluminum layer as the cathode in a sequence through a shadow mask at 10⁻⁶ mbar to form 21 mm² pixels. The thicknesses of all evaporated layers was controlled by a quartz micro-balance resonator pregraduated by profilometry.

Measurements of the OLED characteristics were performed in the N₂ glovebox without encapsulation. The electroluminescence spectra were obtained with an Instrument Systems CAS 120 Array spectrometer sensitive within 200–1100 nm. Current-voltage characteristics were measured by using Keithley 2400 source-meter measurement unit. The turn-on voltage was defined as the voltage at which 1 cd/m² EL intensity was achieved.

2.2. Synthesis

Synthesis of Eu(dbm)₃DPPZ. A solution of 1 mmol of EuCl₃·6H₂O in 20 mL of ethanol was added to a mixture of Hdbm (3 mmol), Et₃N (3 mmol) in 20 mL of ethanol, then a solution of DPPZ (1 mmol) in 30 mL of ethanol was added, and the precipitation was observed. The reaction mixture was stirred for 2 h, then the precipitate was filtered off, washed with cold ethanol, and dried in air.

Synthesis of Eu(tta)₃DPPZ. A solution of 1 mmol of EuCl₃·6H₂O in 20 mL of ethanol was added to a mixture of Htta (3 mmol), Et₃N (3 mmol) in 20 mL of ethanol, then a solution of DPPZ (1 mmol) in 30 mL of ethanol was added, and the precipitation was observed. The reaction mixture was stirred for 2 h, then the precipitate was filtered off, washed with cold ethanol, and dried in air.

Synthesis of Eu(btfa)₃DPPZ. A solution of 1 mmol of EuCl₃·6H₂O in 20 mL of ethanol was added to a mixture of Hbtfa (3 mmol), Et₃N (3 mmol) in 20 mL of ethanol, then a solution of DPPZ (1 mmol) in 30 mL of ethanol was added, and the precipitation was observed. The reaction mixture was stirred for 2 h, then the precipitate was filtered off, washed with cold ethanol, and dried in air.

A single crystal of Eu(btfa)₃DPPZ was obtained by the slow evaporation of the Eu(btfa)₃DPPZ solution in ethanol at room temperature.

3. Results and Discussion

3.1. Synthesis and Characterization

Mixed-ligand complexes Eu(dik)₃DPPZ were synthesized as in [17]. A single crystal of [Eu(btfa)₃DPPZ] was obtained by slow evaporation of the ethanol solution of Eu(btfa)₃DPPZ (Figure 1b). The complex is monomeric, and the Eu³⁺ central ion is surrounded by three btfa⁻ anionic ligands and one DPPZ neutral ligand, which results in CN = 8.

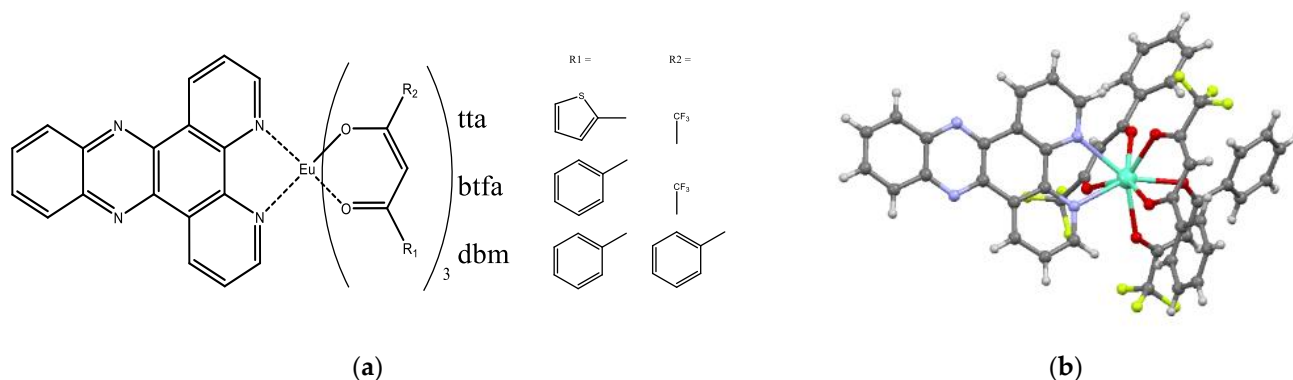


Figure 1. (a) Complexes $\text{Eu}(\text{dik})_3\text{DPPZ}$ used in the present study. (b) The structure of $[\text{Eu}(\text{btfa})_3\text{DPPZ}]$ in crystal.

The PXRD pattern of $\text{Eu}(\text{btfa})_3\text{DPPZ}$ coincided with the one calculated from the $[\text{Eu}(\text{btfa})_3\text{DPPZ}]$ structure (Figure 2b); the PXRD patterns of the other $\text{Eu}(\text{dik})_3\text{DPPZ}$ ($\text{dik} = \text{tta}, \text{dbm}$) coincided with those calculated from the structures of $[\text{Eu}(\text{tta})_3\text{DPPZ}]$ and $[\text{Dy}(\text{dbm})_3\text{DPPZ}]$ (CCDC numbers 2072867 [16] and 1062453, Figure S3). In order to additionally confirm the composition of complexes, ^1H NMR spectroscopy, TGA, and IR spectroscopy were performed (Figures 2a, S1, S2 and S4 in ESI).

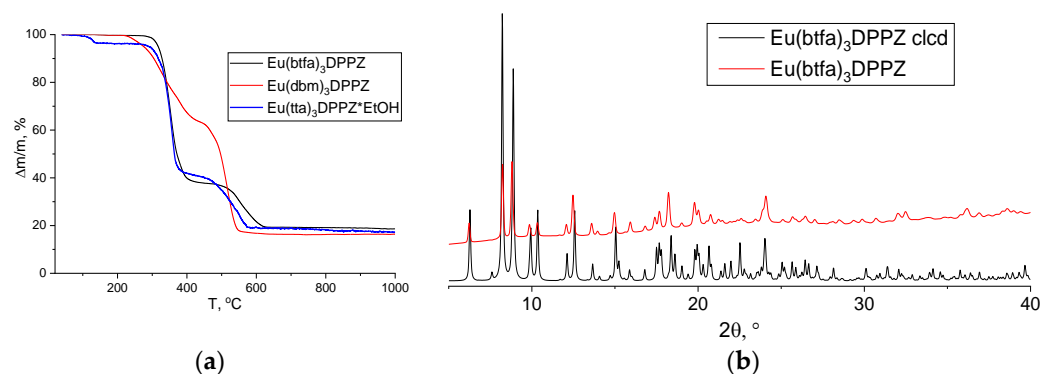


Figure 2. (a) TGA data of $\text{Eu}(\text{btfa})_3\text{DPPZ}$, $\text{Eu}(\text{tta})_3\text{DPPZ}\cdot\text{EtOH}$, and $\text{Eu}(\text{dbm})_3\text{DPPZ}$ powders and (b) PXRD patterns for $\text{Eu}(\text{btfa})_3\text{DPPZ}$: experimental (red curve) and calculated from the crystal structure (black curve).

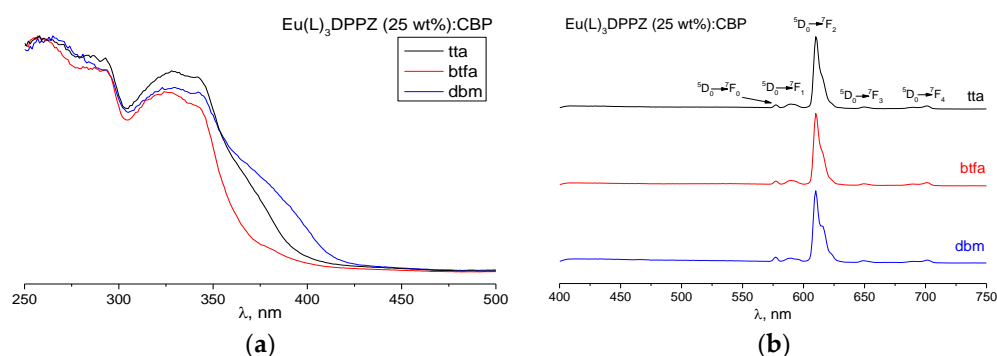
3.2. Photoluminescent Properties

We studied photoluminescent (PL) properties of the complexes' thin films, as well as of the composite films $\text{Eu}(\text{dik})_3\text{DPPZ}:\text{host}$ (Table 1), where the following hosts were selected based on the literature data: 6TCTA:3OXD-7, 6CBP:3OXD-7, 6TCTA:3CBP, and CBP itself [20–22]. Here TCTA is 4,4',4''-tris(carbazol-9-yl)triphenylamine, OXD-7 is 1,3-bis[2-(4-tert-butylphenyl)-1,3,4-oxadiazol-5-yl]benzene, and CBP is 4,4'-Bis(N-carbazolyl)-1,1'-biphenyl.

Table 1. Photoluminescent properties of the Eu(dik)₃DPPZ:host films ($\lambda_{\text{ex}} = 330$ nm).

dik =	Host in Eu(dik) ₃ DPPZ:host	PLQY, %	τ_{obs} , ms	PLQY/ τ_{obs}
tta	-	0.4	0.07	6
	6TCTA:3OXD-7	2.3	0.25	9
	6CBP:3OXD-7	6.4	0.37	17
	6TCTA:3CBP	10.7	0.34	32
	3CBP	11	0.24	46
btfa	-	1.3	0.10	13
	6TCTA:3OXD-7	2.2	0.24	9
	6CBP:3OXD-7	5.4	0.39	14
	6TCTA:3CBP	4.9	0.31	16
	3CBP	4.6	0.27	17
dbm	-	0.6	0.06	10
	6TCTA:3OXD-7	2.3	0.21	11
	6CBP:3OXD-7	5.1	0.31	16
	6TCTA:3CBP	4.1	0.26	16
	3CBP	3	0.17	18

Both doped and undoped Eu(dik)₃DPPZ films exhibit photoluminescence typical of europium ions; the organic photoluminescence is absent (Figures 3 and S5–S7 in ESI). The excitation spectra demonstrate broad excitation bands through the dik[−] (250–300 nm) and the DPPZ (300–400 nm) and are almost unaffected by the host [23].

**Figure 3.** (a) Excitation and (b) photoluminescence spectra of Eu(dik)₃DPPZ thin films doped into CBP: Eu(dik)₃DPPZ, dik = dbm (blue), btfa (red), and tta (black).

The PLQY and observed lifetime (τ_{obs}) values strongly depend on the host. This demonstrates the importance of the measurements of the photophysical data within the composite film even if the properties of the pure compound are known. Such dependence may be associated with the participation of the host in the sensitization process. Indeed, as DPPZ demonstrates low sensitization efficiency and even quenching of the Eu photoluminescence, the presence of the host, able to sensitize its photoluminescence, may affect the photoluminescence efficiency.

At the same time, as both the lifetimes and the PLQY increase, we calculated the PLQY/ τ_{obs} parameter to compare the obtained films. Indeed, the increase of the PLQY linearly increases the electroluminescence intensity, while the increase of the τ_{obs} results in its linear decrease. Thus, the larger PLQY/ τ_{obs} is, the better should be the performance. Interestingly, the PLQY/ τ_{obs} value did not change much after the doping, though it increases in some hosts, and decreases in others. This data demonstrates that according to the photophysical characteristics, CBP can be considered the best host material among the selected ones.

For CBP, as well as for CBP:TCTA, we also studied the dependence of the composite films' photophysical properties on the solvent, from which it was deposited (Table 2). We selected dichloromethane (DCM), tetrahydrofuran (THF), and toluene (Tol) as the most

suitable solvents for solution deposition according to the literature data. The photophysical properties' dependence on the dopant concentration was also studied.

Table 2. The solvent dependence of the photophysical properties of the $\text{Eu}(\text{tta})_3\text{DPPZ}$ -doped films.

Solvent	$\text{Eu}(\text{tta})_3\text{DPPZ}$: CBP:TCTA	PLQY, %	τ_{obs} , ms	PLQY/ τ_{obs}	$\text{Eu}(\text{tta})_3\text{DPPZ}$: CBP	PLQY, %	τ_{obs} , ms	PLQY/ τ_{obs}
DCM	1:(7/3):1	4.0	0.20	20	1:1	2.5	0.15	17
	1:3.5:1.5	7.0	0.29	24	1:2	2.7	0.18	15
	1:7:3	9.7	0.34	29	1:3	3.0	0.20	15
THF	1:(7/3):1	5.0	0.24	21	1:1	4.3	0.18	24
	1:3.5:1.5	9.8	0.33	30	1:2	8.2	0.21	39
	1:7:3	10.7	0.34	32	1:3	11.0	0.24	46
Tol	1:(7/3):1	2.2	0.14	16	1:1	1.6	0.10	16
	1:3.5:1.5	3.6	0.21	17	1:2	3.9	0.16	24
	1:7:3	4.8	0.26	19	1:3	5.3	0.19	28

It revealed that the PLQY values, as well as the τ_{obs} and PLQY/ τ_{obs} values, do indeed strongly depend on the solvent. Thus, the PLQY and PLQY/ τ_{obs} values are lower in the high-boiling toluene than in DCM and THF. This is likely due to the quenching by the residual solvent, which remains within the film even after the thermal treatment.

The comparison of the obtained data demonstrates that the best performance is demonstrated by the $\text{Eu}(\text{tta})_3\text{DPPZ}$:CBP = 1:3 film, deposited from THF.

3.3. OLED Fabrication

Based on the obtained data, OLEDs S1–S3 with the heterostructure ITO/PEDOT:PSS/poly-TPD/EML/TPBi/LiF/Al (TPBi = 2,2',2''-(1,3,5-benzinetriyl)-tris(1-phenyl-1-H-benzimidazole)) were obtained (Figure 4), where spin-coated $\text{Eu}(\text{dik})_3\text{DPPZ}$:CBP 1:3 films served as the EML (dik = tta for S1, btfa for S2, dbm for S3).

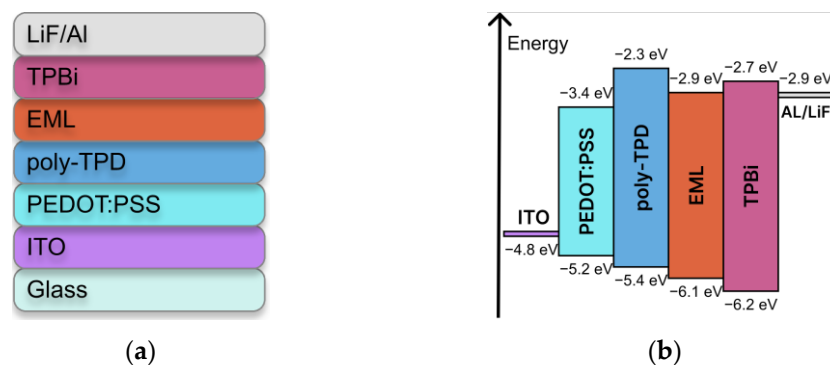


Figure 4. (a) Heterostructure and (b) band structure of OLEDs.

All the diodes demonstrated the pure EL of the europium ion (Figure S8) with CIE coordinates ($x = 0.66$, $y = 0.32$), which coincided exactly with their photoluminescence spectra (Figure 3); their luminance reached up to 700 cd/m^2 (Figure 5). This is one of the highest values obtained so far for solution-deposited Eu-based OLEDs, and it is a result of the purposeful selection of not only the emitter but also the deposition conditions.

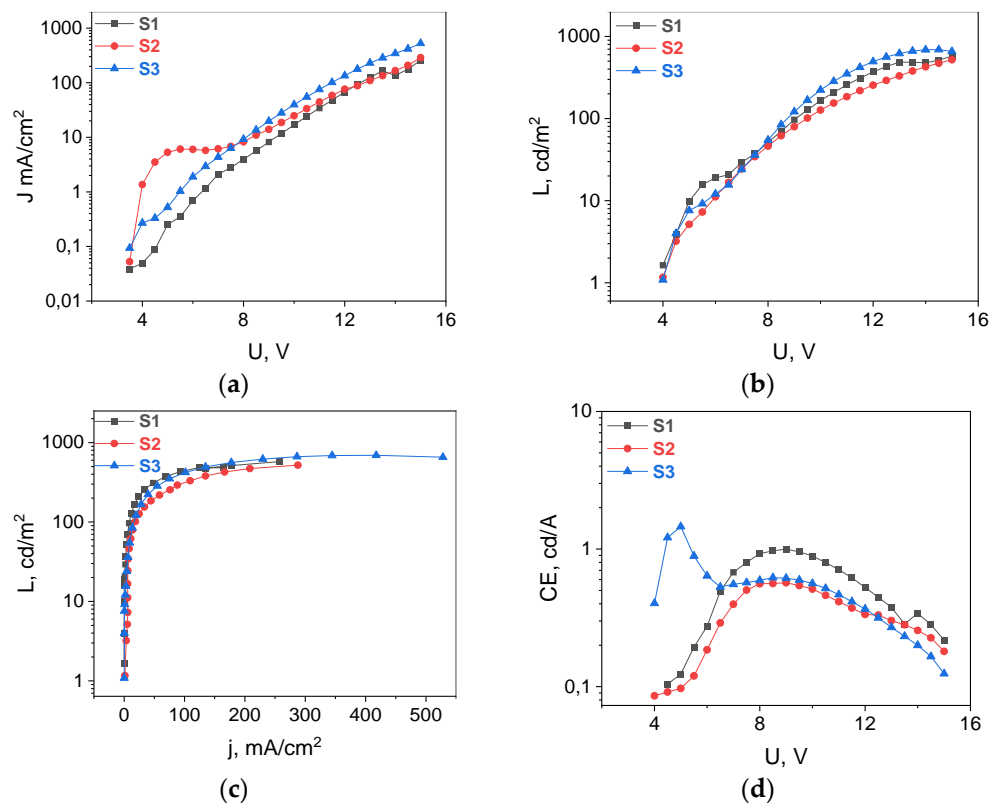


Figure 5. (a) J-V, (b) L-V, (c) L-J, and (d) CE-V curves of Eu(dik)₃DPPZ:CBP 1:3 thin films: dbm (blue), btfa (red), and tta (black).

OLED degradation and stability is an important issue, which has never been studied for lanthanide-based OLEDs. In the present work, the stability was studied for the OLED S1 at 7 V and 8.6 V (starting efficiency of ca. 10 cd/m² and 100 cd/m², respectively).

At both voltages, an interesting phenomenon was observed (Figure 6): upon measurement, first, an increase in intensity was observed, which reached 33% at 7 V; after 25 s, the intensity increased from 14 cd/m² to 18.66 cd/m². This is quite unusual and may be connected with the further solvent elimination from the layer or heating up of the OLED device. Thus, the obtained maximum intensity, t_{50} of 10,643 s = 177.3 min ~ 3 h, was measured, while from the initial value of 14 cd/m², t_{50} has not even been reached after 12,000 s.

At 8.6 V, the intensity increase is not that pronounced. From the initial intensity, t_{50} of 1971 s ~ 33 min was reached. These values are quite remarkable for the lanthanide-based solution-processed OLEDs.

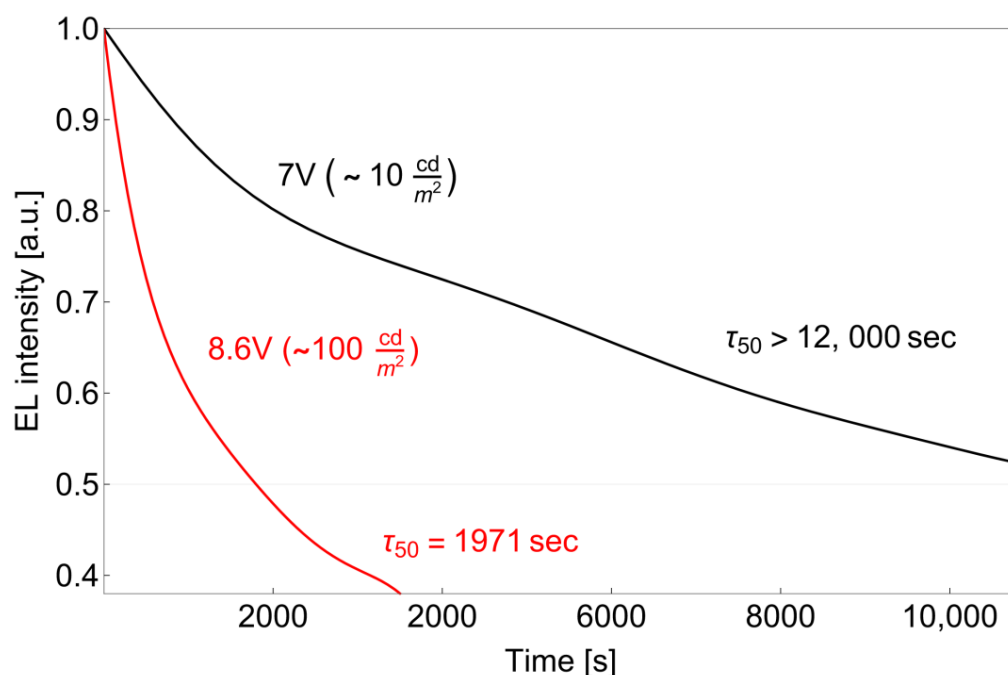


Figure 6. Lifetime of solution-processed OLED based on $\text{Eu}(\text{dbm})_3\text{DPPZ}$ under the constant voltage of 7 V ($\sim 10 \text{ cd/m}^2$) and 8.6 V ($\sim 100 \text{ cd/m}^2$).

4. Conclusions

We demonstrated the strong dependence of the photophysical properties of composite films containing europium complexes on the composition, such as host and doping concentration, as well as deposition parameters. The optimization of these parameters allowed us to obtain the films with the highest PLQY/τ ratio, i.e., films doped into CBP, deposited from the THF. These films were tested in OLEDs, and a luminance of up to 700 cd/m^2 was obtained thanks to the purposeful selection of the deposition conditions, with $t_{50} \sim 33 \text{ min}$ at 100 cd/m^2 . This is the first study of lanthanide-based OLED stability.

Supplementary Materials: The following supporting information can be downloaded at: <https://www.mdpi.com/article/10.3390/ma16030959/s1>: Figure S1. (a) TGA curve of $\text{Eu}(\text{tta})_3\text{DPPZ}\cdot\text{EtOH}$. Normalized ionic currents are shown in blue ($m/z = 18$), red ($m/z = 44$), and green ($m/z = 46$). (b) IR-spectrum of $\text{Eu}(\text{tta})_3\text{DPPZ}\cdot\text{EtOH}$. (c) TGA curves of $\text{Eu}(\text{btfa})_3\text{DPPZ}$ and $\text{Eu}(\text{dbm})_3\text{DPPZ}$; Figure S2. The ^1H NMR spectra of the $\text{Eu}(\text{tta})_3\text{DPPZ}$ and DPPZ in DMSO- d_6 solution. Figure S3. Top: PXRD data of $\text{Eu}(\text{dbm})_3\text{DPPZ}$ in comparison to the theoretical PXRD, obtained from the single crystal data of $\text{Dy}(\text{dbm})_3\text{DPPZ}$ (left) and indexed PXRD pattern of $\text{Eu}(\text{tta})_3\text{DPPZ}\cdot\text{EtOH}$. Bottom: Molecules in the structures of $\text{Eu}(\text{tta})_3\text{DPPZ}$ (left) and $\text{Eu}(\text{btfa})_3\text{DPPZ}$. Figure S4. IR spectra of (a) $\text{Eu}(\text{btfa})_3\text{DPPZ}$, (b) $\text{Eu}(\text{dbm})_3\text{DPPZ}$, and (c) $\text{Eu}(\text{tta})_3\text{DPPZ}\cdot\text{EtOH}$. Figure S5. (a) Photoluminescence and (b) excitation spectra of pure thin films. Figure S6. Excitation spectra of composite thin films. Figure S7. Photoluminescence spectra of composite thin films. Figure S8. Electroluminescence spectra of OLEDs S1–S3.

Author Contributions: Conceptualization, V.V.U.; methodology, V.V.U., S.V.M., and M.I.K.; investigation, M.I.K., K.M.K., A.B., M.S., E.I.; resources, V.V.U., A.S.G., S.V.M., and M.S.; data curation, V.V.U.; writing—original draft preparation, V.V.U., M.I.K., A.B., E.I., and K.M.K.; writing—review and editing, V.V.U., A.S.G., M.S., and M.I.K.; funding acquisition, V.V.U. All authors have read and agreed to the published version of the manuscript.

Funding: We thank the Grants Council of the President of the Russian Federation (President's grant MD-2821.2021.1.3) for funding. Photophysical studies were financed by the Russian Science Foundation (grant 20-73-10053). X-ray diffraction data were supported by the Ministry of Science and Higher Education of the Russian Federation using the equipment of the Center for molecular composition studies of A.N. Nesmeyanov Institute of Organoelement Compounds.

Institutional Review Board Statement: Not applicable.

Informed Consent Statement: Not applicable.

Data Availability Statement: Data available on request.

Acknowledgments: The authors are thankful to the company FlexLab LLC for providing consumables and facilities for OLED fabrication.

Conflicts of Interest: The authors declare no conflict of interest.

References

1. Jung, S.O.; Zhao, Q.; Park, J.-W.; Kim, S.O.; Kim, Y.-H.; Oh, H.-Y.; Kim, J.; Kwon, S.-K.; Kang, Y. A Green Emitting Iridium(III) Complex with Narrow Emission Band and Its Application to Phosphorescence Organic Light-Emitting Diodes (OLEDs). *Org. Electron.* **2009**, *10*, 1066–1073. [[CrossRef](#)]
2. Schwartz, G. Flexible Polymer Transistors with High Pressure Sensitivity for Application in Electronic Skin and Health Monitoring. *Nat. Commun.* **2013**, *4*, 1859. [[CrossRef](#)] [[PubMed](#)]
3. Smith, J.T.; O'Brien, B.; Lee, Y.-K.; Bawolek, E.; Christen, J.B. Application of Flexible OLED Display Technology For Electro-Optical Stimulation and/or Silencing of Neural Activity. *J. Disp. Technol.* **2014**, *10*, 514–520. [[CrossRef](#)]
4. Lochner, C.M.; Khan, Y.; Pierre, A.; Arias, A.C. All-Organic Optoelectronic Sensor for Pulse Oximetry. *Nat. Commun.* **2014**, *5*, 5745. [[CrossRef](#)] [[PubMed](#)]
5. Golovynskyi, S.; Golovynska, I.; Stepanova, L.; Datsenko, O.; Liu, L.; Qu, J.; Ohulchanskyi, T. Optical Windows for Head Tissues in near and Short-Wave Infrared Regions: Approaching Transcranial Light Applications. *J. Biophotonics* **2018**, *11*, e201800141. [[CrossRef](#)] [[PubMed](#)]
6. Sastri, V.R.; Perumareddi, J.R.; Rao, V.R.; Rayudu, G.V.S.; Bünzli, J.C. *Modern Aspects of Rare Earths and Their Complexes*; Elsevier: Amsterdam, The Netherlands, 2003.
7. Valentina, V. Utochnikova Lanthanide Complexes as OLED Emitters. In *Handbook on the Physics and Chemistry of Rare Earths*; Bünzli, J.-C.G., Pecharsky, V., Eds.; Elsevier B.V.: Amsterdam, The Netherlands, 2021.
8. Utochnikova, V.V.; Aslandukov, A.N.; Vashchenko, A.A.; Goloveshkin, A.S.; Alexandrov, A.A.; Grzibovskis, R.; Bünzli, J.C.G. Identifying Lifetime as One of the Key Parameters Responsible for the Low Brightness of Lanthanide-Based OLEDs. *Dalton Trans.* **2021**, *50*, 12806–12813. [[CrossRef](#)] [[PubMed](#)]
9. Xu, H.; Sun, Q.; An, Z.; Wei, Y.; Liu, X. Electroluminescence from Europium(III) Complexes. *Coord. Chem. Rev.* **2015**, *293–294*, 228–249. [[CrossRef](#)]
10. Ma, D.; Qiu, Y.; Duan, L. Vacuum-Deposited versus Spin-Coated Emissive Layers for Fabricating High-Performance Blue–Green-Emitting Diodes. *Chempluschem* **2018**, *83*, 211–216. [[CrossRef](#)]
11. Ge, Z.; Hayakawa, T.; Ando, S.; Ueda, M.; Akaike, T.; Miyamoto, H.; Kajita, T.; Kakimoto, M.A. Spin-Coated Highly Efficient Phosphorescent Organic Light-Emitting Diodes Based on Bipolar Triphenylamine-Benzimidazole Derivatives. *Adv. Funct. Mater.* **2008**, *18*, 584–590. [[CrossRef](#)]
12. Lee, T.-W.; Noh, T.; Shin, H.-W.; Kwon, O.; Park, J.-J.; Choi, B.-K.; Kim, M.-S.; Shin, D.W.; Kim, Y.-R. Characteristics of Solution-Processed Small-Molecule Organic Films and Light-Emitting Diodes Compared with Their Vacuum-Deposited Counterparts. *Adv. Funct. Mater.* **2009**, *19*, 1625–1630. [[CrossRef](#)]
13. Deng, L.; Li, W.; Li, J. Efficient Bluish-Green Phosphorescent Iridium Complex for Both Solution-Processed and Vacuum-Deposited Organic Light-Emitting Diodes. *Displays* **2013**, *34*, 413–417. [[CrossRef](#)]
14. Mao, G.; Wu, Z.; He, Q.; Jiao, B.; Xu, G.; Hou, X.; Chen, Z.; Gong, Q. Considerable Improvement in the Stability of Solution Processed Small Molecule OLED by Annealing. *Appl. Surf. Sci.* **2011**, *257*, 7394–7398. [[CrossRef](#)]
15. Feng, S.; Duan, L.; Hou, L.; Qiao, J.; Zhang, D.; Dong, G.; Wang, L.; Qiu, Y. A Comparison Study of the Organic Small Molecular Thin Films Prepared by Solution Process and Vacuum Deposition: Roughness, Hydrophilicity, Absorption, Photoluminescence, Density, Mobility, and Electroluminescence. *J. Phys. Chem. C* **2011**, *115*, 14278–14284. [[CrossRef](#)]
16. Kuznetsov, K.M.; Kozlov, M.I.; Aslandukov, A.N.; Vashchenko, A.A.; Medved'ko, A.V.; Latipov, E.V.; Goloveshkin, A.S.; Tsymbarenko, D.M.; Utochnikova, V.V. Eu(Tta)3DPPZ-Based Organic Light-Emitting Diodes: Spin-Coating vs. Vacuum-Deposition. *Dalton Trans.* **2021**, *50*, 9685–9689. [[CrossRef](#)] [[PubMed](#)]
17. Sun, P.P.; Duan, J.P.; Lih, J.J.; Cheng, C.H. Synthesis of New Europium Complexes and Their Application in Electroluminescent Devices. *Adv. Funct. Mater.* **2003**, *13*, 683–691. [[CrossRef](#)]
18. Coelho, A.A. Indexing of Powder Diffraction Patterns by Iterative Use of Singular Value Decomposition. *J. Appl. Crystallogr.* **2003**, *36*, 86–95. [[CrossRef](#)]
19. Bruker, *TOPAS 4.2 User Manual*; Bruker AXS GmbH: Karlsruhe, Germany, 2009.
20. Giroto, E.; Pereira, A.; Arantes, C.; Cremona, M.; Bortoluzzi, A.J.; Salla, C.A.M.; Bechtold, I.H.; Gallardo, H. Efficient Terbium Complex Based on a Novel Pyrazolone Derivative Ligand Used in Solution-Processed OLEDs. *J. Lumin.* **2019**, *208*, 57–62. [[CrossRef](#)]
21. Biju, S.; Xu, L.J.; Hora Alves, M.A.; Freire, R.O.; Chen, Z.N. Bright Orange and Red Light-Emitting Diodes of New Visible Light Excitable Tetrakis-Ln-β-Diketonate (Ln = Sm³⁺, Eu³⁺) Complexes. *New J. Chem.* **2017**, *41*, 1687–1695. [[CrossRef](#)]

22. Zhang, X.; Guo, X.; Chen, Y.; Wang, J.; Lei, Z.; Lai, W.; Fan, Q.; Huang, W. Highly Efficient Red Phosphorescent Organic Light-Emitting Devices Based on Solution-Processed Small Molecular Mixed-Host. *J. Lumin.* **2015**, *161*, 300–305. [[CrossRef](#)]
23. Wu, F.; Mao, M.; Cen, Y.; Yang, H.; Qin, Z.; Ma, L. Copolymerization of Eu(TTA)₃Phen Doped Styrene and Methyl Methacrylate Nanoparticles and Use in Quantitative Detection of Pepsinogen. *RSC Adv.* **2017**, *7*, 12217–12223. [[CrossRef](#)]

Disclaimer/Publisher's Note: The statements, opinions and data contained in all publications are solely those of the individual author(s) and contributor(s) and not of MDPI and/or the editor(s). MDPI and/or the editor(s) disclaim responsibility for any injury to people or property resulting from any ideas, methods, instructions or products referred to in the content.